UNIVERSITY OF ZAGREB
FACULTY OF ELECTRICAL ENGINEERING AND COMPUTING

MASTER THESIS No. 1286

Detectability of Patient Zero Depending on its Position in the Network

Iva Miholić

Zagreb, May 2016.

Umjesto ove stranice umetnite izvornik Vašeg rada.

Da bi ste uklonili ovu stranicu obrišite naredbu `\izvornik`*.*

CONTENTS

List of Figures

LIST OF ALGORITHMS

1. Introduction

A *network* is a set of items with connections between them. The Internet, the World Wide Web, social networks like genealogical trees, networks of friends or co-workers, biological networks like epidemiological networks, networks of citations between papers, distribution systems like postal delivery routes: they all take a form of networks. Most social, biological and technological networks have specific structural properties. Such networks are referred to as *complex networks*. An example of a complex network is represented on Figure 1.1.

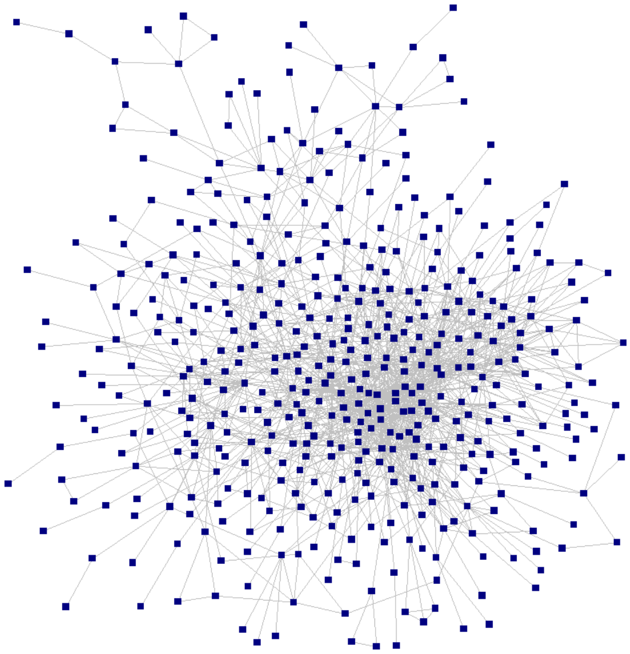

Figure 1.1: A network graph of Paul Erdõs and his collaborators, courtesy of Krebs [1]. The nodes represent mathematicians and the edges represent the relationship "wrote a paper with".

A network structure or a topology can be mathematically modelled as a graph with set of vertices (or nodes) representing the items of the network. The network structure can then be analysed using graph theory. An edge between two nodes represents a connection between the two corresponding items. Edges can be directed or undirected, depending on the nature of the connection. To better mimic the real-world (complex) network structure, it is common to add attributes to nodes and/or edges or to have both directed and undirected edges on the same graph.

For large-scaled complex networks that have millions or billions of vertices, the study in the form of traditional graph theory is not sufficient or sometimes possible. When this is the case, the statistical methods for quantifying large complex networks are used.

The ultimate goal of the study of complex network structure is to understand and explain the workings of systems built upon network such as spreading of disease or information propagation.

After statistical properties analysis, the model of the system or a process is created. The model can help us understand the meaning of statistical properties - how they came to be as they are and how they relate to the behaviour of a networked system. Based on the statistical properties and using the right model, the behaviour of networked systems can be determined and predicted.

The basis of the complex network theory – the structure analysis and the process modelling – can be found in Newman [2].

1.1. Epidemic processes in complex networks

The models for stochastic processes such as disease spreading are categorized as homogeneous or heterogeneous mixing frameworks. The former assume that all individuals in a population have an equal probability of contact and different equations can be applied to understand epidemic dynamics. Since such models fail to describe the realistic scenario of disease spreading, heterogeneity is introduced by using a network structure.

There is an extremely close relationship between epidemiology and network theory since the connections between individuals (or group of individuals) allowing an infectious disease to propagate naturally define a contact network. Simplest epidemic dynamics consider a system with fixed total population consisting of N individuals modelled with undirected contacting network. We define the contact network as an undirected and non-weighted graph $G(N, L)$ with fixed set of nodes N and fixed set of links L. A link (u, v) between two nodes exists if the two corresponding members were in contact during the epidemic time.

The structure of the network has profound impact on the contagnion dynamics but in order to understand the evolution of the epidemic over time we have to define the basic individual-level processes that govern the epidemic spreading. Complementary to the network, epidemic modelling describes the dynamical evolution of the contagion process within a population. The state of the art results on epidemic modelling in complex networks can be found in Pastor-Satorras et al. [3].

Classic epidemic models generally assume the network is static during epidemic process while the population can be divided into different classes or compartments depending on the stage of the disease, such as susceptible (those who can contract the infection), infectious (those who contracted the infection and are contagious), recovered, removed or immune. The model defines the basic processes that govern the transition of individuals from one compartment to another. Each member of population can be a part of exactly one compartment at once.

Understanding the structure of the transmission network along with choosing the right epidemic model allows us to predict the distribution of infection and to simulate the full dynamics in order to control disease or plan immunization. In this thesis we will focus on SIR model for epidemic spreading and its modification, the ISS model for modelling rumour diffusion.

1.2. Finding patient zero

The inverse problem of estimating the initial epidemic conditions like localizing the source of an epidemic, commonly known as the patient zero problem, has only recently been formulated.

In the patient zero problem the source(s) of an epidemic or information diffusion propagation are determined based on limited knowledge of network structure or partial history of the propagation. The survey of methods for identifying the propagation source in networks can be found in Jiang et al. [4].

In the case of the SIR model there are three different approaches. Zhu and Ying [5] proposed a simple path counting approach and prove that the source node minimizes the maximum distance (Jordan centrality) to the infected nodes on infinite trees. Lokhov et al. [6] used a dynamic message-passing algorithm and estimate the probability that a given node produces the observed snapshot using a mean-field approch and an assumption of a tree-like contact network.

Antulov-Fantulin et al. [7] introduce analytical combinatoric, as well as Monte-Carlo based methods for source detection problem. These methods produce exact and approximate source probability distribution for any network topology based on a snapshot of the epidemic at known discrete time T. The provided benchmark results show

Monte-Carlo based MAP estimators outperforming previous results on a grid network for the SIR model. Additionally, they are applicable to many heterogeneous mixing models (SIR, IS, ISS) and are able to introduce uncertainty in the epidemic starting time, as well as uncertainty of temporal ordering of interactions. Even though the introduced Monte Carlo methods assume the epidemic started from a single source, one can also discriminate such hypothesis using Kolmogorov-Smirnov test.

1.3. Effects of network topology on epidemic spreading and detectability of patient zero

Complex networks show various levels of correlations in their topology which can have an impact on dynamical processes running on top of them. Real-world network of relevance for epidemic spreading are different from regular lattices. Networks are hierarchically organized with a few nodes that may act as hubs and where the vast majority of nodes have few interactions. Although randomness in the connection process of nodes is always present, organizing principles and correlations in the connectivity patterns define network structures that are deeply affecting the evolution and behavior of epidemic and contagion process. These network's complex features often find their signature in statistical distributions which are generally heavy tailed and skewed.

Antulov-Fantulin et al. [7] have also introduced a metric for source detectability based on the entropy of estimated source probability distribution. The detectability of source node differs based on models parameters concerning the rate of disease spreading. Since topological properties of the network have profound impact on epidemic dynamic, the detectability of source node depending on its topological properties is in the focus of this thesis.

1.4. Structure of the thesis

In Chapter 2 ...

In Chapter 3 the SIR epidemic model as well as ISS model for rumour diffusion are introduced and the algorithms for their simulation in discrete time are presented.

Chapter 4 introduces Direct Monte Carlo and Soft Margin Monte Carlo algorithms [7] for indetification of patient zero.

In Chapter 5 the technique of importance sampling is used to create the Sequential Importance Sampling (SIS) algorithm - a new algorithm for single source detection problem. A few reduction based optimization techniques are also introduced.

Chapter 6 uses benchmark data from [7] to assert accuracy of Direct Monte Carlo and Soft Margin implementations. Detailed analysis of SIS algorithm performance is also given.

In Chapter 7 detectability of source node based on parameters of SIR and ISS model is revisited. The detectability analysis for $1-$Barabasi and Erdos Renyi sample graphs is given, as well as the detectability breakdown based on nodes attributes: degree, k-core, betweenness centrality and eigenvector centrality.

2. Complex network structure

Most of real networks in social and biological systems are characterized by the similar topological properties: small average path length, high clustering coefficients, fat tailed scale-free degree distributions, degree correlations and local network structure observable as the presence of communities.

The small world network property is considered to be present when average shortest path length is comparable to logarithm of the network size.

The **degree distribution** $P(k)$ defines the probability of choosing the vertex with degree k uniformly from the set of all vertices. The power-law degree distribution of the form $P(k) = Ak^{-\gamma}$ where $2 < \gamma < 3$ can be fitted to degree distributions of most real networks. The networks with such property are refered to as *scale-free networks*.

2.1. Measures and metrics

The adjacency matrix A of network with N nodes is a matrix of size $N \times N$ which contains non-zero element A_{ij} if there exist an edge between vertices i and j. For the unweighted network all non-zero elements are equal to one. Note the adjacency matrix is symmetric for undirected graphs and generally asymmetric for directed graphs.

2.1.1. Degree

2.1.2. K-core

A path in a network is defined as an arbitrary sequence of vertices in which each pair of adjacent vertices are directly connected in the graph. Number of different paths between two vertices i and j can be computed from the $0 - 1$ adjacency matrix as A_{ij}^k. The number of different cycles of length k can thus be computed as the sum $\sum_{m \in V} A_{mm}^k$ - exactly the trace of the matrix A^k.

A geodesic path is the shortest path between two vertices. Let d_{ij} denote the length of geodesic path from vertex i to vertex j.

The **closeness centrality** C_i of vertex v_i is the harmonic mean between the distances of geodesic paths from the vertex v_i to all others:

$$C_i = \frac{1}{n-1} \sum_{j \neq i} \frac{1}{d_{ij}}.$$

Let σ_{st} be the number of geodesic paths between pairs of vertices v_s and v_t and let $\sigma_{st}(v_i)$ be the number of the geodesic paths σ_{st} which pass through the vertex v_i. The **betweenness centrality** is than defined as

$$C(v_i) = \sum_{st} \frac{\sigma_{st}(v_i)}{\sigma_{st}}$$

.

Eigenvector centrality [8] captures a concept the vertex is more important if it has more important neighbours. For the given vertex v, the eigenvector centrality is defined recursively as

$$x_v = \sum_k A_{vk} x_k$$

where A is the adjacency matrix. Consequently, the only x_k we are interested in are the neighbours of x_v.

Centralities x_v can be calculated iteratively, starting from arbitrary vector $\vec{x}(0) = \{x_1(0), x_2(0), \ldots, x_N(0)\}$ using equality $\vec{x}(t) = A^t \vec{x}(0)$.

2.2. Modelling global network structure

2.2.1. Erdõs-Renyi graph model

2.2.2. Barabasi-Albert graph model

Barabasi-Albert model is the model of evolving a scale-free network, which uses a preferential attachment [9] property. Starting from m_0 isolated vertices, at each time step new vertices with m edges are added to the netowrk $m < m_0$. The new vertex will create an edge to the existing node v_i with the probability proportional to its degree k_i. The Barabasi-Albert graph model produces power law distribution $P(k) \approx k^{-3}$ in the limit of time. The average geodesic path increases logarithmically with the size of the network.

3. Epidemic process modelling

In the focus of this thesis are heterogeneous epidemic models on the contact network formed by connections between single contacting individuals with transitions of individuals between compartments happening in discrete time steps.

3.1. SIR model

Wide range of diseases that provide immunity to the host can be successfully modelled on a network whose members take one of three possible roles at a time: susceptible (S), infected (I) or recovered (R). The diffusion of disease takes place between infected nodes and their susceptible neighbours. An infectious node may also recover from the disease. The recovery grants permanent immunity effectively erasing the member from the contacting network. The possible events can be represented as

$$S + I \xrightarrow{p} 2I, \qquad I \xrightarrow{q} R. \tag{3.1}$$

In the SIR model, the infection and recovery process completely determine the epidemic evolution. The transitions (3.1) occur spontaneously and independently in each time step. In discrete-time formulation an infected individual when meeting susceptible will infect the neighbouring susceptible with probability p at each time step. The recovery probability q is the probability infected individual will recover at any time step. The transition probabilities p and q are often assumed constant and equal for all nodes in the same epidemic process.

3.1.1. Simulating the discrete SIR epidemic

For the contacting network represented by $G(N, L)$ and SIR parameters p and q, we are able to simulate one time step of discrete SIR process. Let s_t, i_t and r_t denote sets of nodes that are respectively susceptible, infected and recovered after time step t. At time step t all previously infected nodes i_{t-1} will try to infected their susceptible neighbours independently of each other and at the same time. Afterwards the passive recovery process will try to turn them to recovering nodes, each with probability q.

This process can be simulated with NaiveSIR algorithm [10] by putting all the initially infected nodes in the queue. While traversing the nodes, we try to infect each neighbouring node. If the node gets infected, it gets pushed to the queue. SIR simulation of one time step t is described by algorithm 1.

Algorithm 1: One time step NaiveSIR simulation on graph G.

```
Data: G - network, $(p, q)$ -parameters of the SIR model, $Iq$ - queue of infected
      nodes, $I$ - bitset of infected nodes, $S$ - bitset of susceptible nodes, $R$ -
      bitset of recovered nodes
infected_size = $Iq$.size();
while (!$Iq$.empty() and infected_size > 0) do
    infected_size $=$ infected_size $-1$;
    $u = Iq$.front();
    $Iq$.pop();
    foreach $v \in$ G.adj_list($u$) do
        if $v \in S$ then
            let transmission $u \rightarrow v$ occur with probability $p$;
            if $u \rightarrow v$ occured then
                update($I(v)$ and $S(v)$);
            end
    end
    let transmission $u \rightarrow v$ occur with probability $q$;
    if $u \rightarrow v$ occured then
        update($I(u)$ and $R(u)$);
    else
        Iq.insert(u);
    end
end
return {S, I, R}
```

3.1.2. Probability of one time step transition

Probability of one time step transition can be easily evaluated. Let $nei(v)$ indicate a set of all neighbours of node v, $nei(V)$ a set of all neighbours of all nodes in set V and

$nei_V(v) = nei(v) \cap V$, a set of all neighbours of v that are also in V. After k-th time step of the SIR process, the resulting i_k and r_k were given. At time step k, only initially active nodes i_{k-1} and their neighbours $nei(i_{k-1})$ actively participate in the epidemic process. For each node v in $i_{k-1} \cup nei(i_{k-1})$, one of four independent events may have happened during time step k:

- E_1 : **if** $v \notin i_{k-1}$ and $v \in i_k$
  node v was infected with probability $1 - (1-p)^{nei_{i_{k-1}}(v)}$
- E_2 : **if** $v \notin i_{k-1}$ and $v \notin i_k$
  node v was not infected with probability $(1-p)^{nei_{i_{k-1}}(v)}$
- E_3 : **if** $v \in i_{k-1}$ and $v \notin r_k$
  node v was recovered with probability q
- E_4 : **if** $v \in i_{k-1}$ and $v \in r_k$
  node v was not recovered with probability $1 - q$

Since all the events are independent and the sets corresponding to events $E_1 - E_4$ are disjoint while completely covering the set of active nodes $i_{k-1} \cup nei(i_{k-1})$, the conditional probability of the one time step SIR transition $P(i_k, r_k | i_{k-1}, r_{k-1})$ can be calculated as

$$\begin{aligned} P(i_k, r_k | i_{k-1}, r_{k-1}) = & \left[\Pi_{v \in E_1} (1 - (1-p)^{nei_{i_{k-1}}(v)})\right] \left[\Pi_{v \in E_2} (1-p)^{nei_{i_{k-1}}(v)}\right] \\ & \cdot \left[\Pi_{v \in E_3} q\right] \left[\Pi_{v \in E_4} (1-q)\right] \end{aligned} \tag{3.2}$$

where $nei_{i_{k-1}}(v)$ is the set of all neighbours of nodes i_{k-1} – the ones infected at the beginning of time step k.

3.2. Epidemic models as social contagion processes

Even though infectious diseases represent the central focus of epidemic modelling, the model where an individual is strongly influenced by the interaction with peers is present in several other domains, especially in social context in the diffusion of information, the propagation of rumour and adoption of innovation or behaviours. Since the social contacts can in these domains generate epidemic-like outbreaks, simple models for information diffusion are epidemic models modified to specific features of social contagion. The crucial difference to pathogen spreading is that transmission of information involves intentional acts by both the sender and the receiver and it is often beneficial for both participants.

3.2.1. Rumour spreading with the ISS model

The need to study rumour spreading presents itself in a number of important technological and commercial applications where it is desirable to spread the "epidemic" as fast and as efficient as possible. In examples such as rumour based protocols for resource discovery and marketing campaigns that use rumour like strategies (viral marketing) the problem translates to design of an epidemic algorithm in such a way that the given information reaches as much nodes as possible, similarly to a rumour.

Models for rumour spreading are variants of the SIR model in which the recovery process does not occur spontaneously, but rather is a consequence of interactions. The modification mimics the idea it is worth spreading the rumour as long as it is novel for the recipient. This process can be formalized as a model where each of N members of the contacting network can be a part of one of three compartments: **ignorant (S), spreader (I) and stifler (R)**. Ignorants have not heard the rumour and are susceptible to being informed. Spreaders are actively spreading the rumour, while stiflers know about the rumour but they're not spreading it.

The spreading process evolves by direct contacts of spreaders with others in the population. When a spreader meets an ignorant, the latter turns into a new spreader with probability a. When a spreader meets another spreader or a stifler, the former spreader turns into stifler with probability b and the latter remains unchanged. This model is known as the ISS model (Ignorant-Spreader-Stifler) [11]. The possible events can be represented as

$$S + I \xrightarrow{\alpha} 2I, \quad R + I \xrightarrow{\beta} 2R, \quad 2I \xrightarrow{\beta} R + I.$$

Since we examine the spreading process in discrete time, at each time step, the current spreaders try to interact with their neighbours. A modification of the NaiveSIR algorithm for rumour spreading simulation of one time step t is described by algorithm 2.

Algorithm 2: One time step simulation of rumour spreading under ISS model on graph **G**.

```
Data: G - network, $(a, b)$ - parameters of the ISS model, $Iq$ - priority queue of
      spreader nodes, $I$ - bitset of spreader nodes, $S$ - bitset of ignorant nodes,
      $R$ - bitset of stifler nodes
stifler_size = $Iq$.size();
while (!$Iq$.empty() and stifler_size > 0) do
    stifler_size $=$ stifler_size $-1$;
    $u = Iq$.front();
    $Iq$.pop();
    foreach $v \in$ G.adj_list($u$) do
        if $v \in S$ then
            let transmission $u \to v$ occur with probability $a$;
            if $u \to v$ occured then
                update($I(v)$ and $S(v)$);
            end
        else
            let transmission $u \to v$ occur with probability $b$;
            if $u \to v$ occured then
                update($I(u)$ and $R(u)$);
                break;
            end
    end
    if $u \in I$ then
        Iq.insert(u);
    end
end
return {S, I, R}
```

4. Patient zero – single source epidemic detection

In accordance with [7], we will focus on a patient zero problem given snapshot of population at time T and complete knowledge of underlying contacting network modelled by G with the assumption the epidemic has started from a single source node and that it is governed by the SIR process with known p and q. The estimators proposed in [7] will be presented in this chapter, while the newly proposed estimators based on importance sampling technique will be presented in the next chapter.

Let random vector $\vec{S} = (S(1), \dots, S(N))$ indicate the nodes that got infected up to a predefined temporal threshold T with SIR(p, q) epidemic process on network G with N nodes. $S(i)$ is a Bernoulli random variable with the value 1 if the node i got infected before time T from the start of the epidemic process. We observe one realization $\vec{s}_*$ of $\vec{S}$ and we want to infer which nodes from the set of infected or recovered nodes $\Theta = \{\theta_1, \theta_2, \dots, \theta_m\}$ are the most likely to be the source of the epidemic process. The finite set of possible source nodes Θ is determined by realization $\vec{s}_*$.

A maximum aposteriori probability estimate (MAP) is the node with the highest probability for being the source of the epidemic spread for a given realization $\vec{s}_*$:

$$\hat{\theta}_{MAP} = \text{arg max}_{\theta_i \in \Theta} P(\Theta = \theta_i | \vec{S} = \vec{s}_*) \tag{4.1}$$

By applying the Bayes theorem with equal apriori probabilities $P(\Theta = \theta_i)$, probability in (4.1) can be expressed as

$$\begin{aligned} P(\Theta = \theta_i | \vec{S} = \vec{s}_*) &= \frac{P(\vec{S} = \vec{s}_* | \Theta = \theta_i) P(\Theta = \theta_i)}{\sum_{\theta_k \in \Theta} P(\vec{S} = \vec{s}_* | \Theta = \theta_k) P(\Theta = \theta_k)} \\ &= \frac{P(\vec{S} = \vec{s}_* | \Theta = \theta_i)}{\sum_{\theta_k \in \Theta} P(\vec{S} = \vec{s}_* | \Theta = \theta_k)}. \end{aligned} \tag{4.2}$$

4.1. Direct Monte Carlo estimator

The integration problem

$$\mathbf{E_f}[h(X)] = \int_X h(x)f(x)dx \tag{4.3}$$

can be estimated using Monte Carlo technique with n samples $X_1, \ldots, X_n$ generated from the density f as the empirical average

$$h_n = \frac{1}{n}\sum_{j=1}^{n} h(X_j). \tag{4.4}$$

The convergence of h_n towards $\mathbf{E_f}[h(X)]$ is assured by the Strong Law of Large Numbers.

Inferring the probability $P(\vec{R} = \vec{r}_*|\Theta = \theta_i)$ up to multiplicative constant is an integration problem equivalent to expectation of Kronecker delta function $\delta(\vec{R}) = 1\{\vec{R} = \vec{r}_*\}$ where $\vec{R}$ is a random variable governed by probability $P(\vec{R}|\Theta = \theta_i)$. Let m_i denote estimation of expected number of hits for a fixed source θ_i estimated using Monte Carlo technique:

$$m_i = \sum_{j=1}^{n} 1\{\vec{R}_i = r_*\} \tag{4.5}$$

where $\vec{R}_i$ are drawn from $P(\vec{R}|\Theta = \theta_i)$. With Direct Monte Carlo estimator m_i is obtained by simulating epidemic process up to time T starting from a single infected node θ_i and checking whether the generated realization $\vec{R}_i$ coincides with $\vec{r}_*$. Since m_i is estimation of $P(\vec{R} = \vec{r}_*|\Theta = \theta_i)$ up to multiplicative constant $1/n$ for all $\theta_i \in S$, we derive Direct Monte Carlo MAP estimator based on the estimation of probability $P(\Theta = \theta_i|\vec{R} = \vec{r}_*)$ combining (4.5) with (4.2):

$$\hat{P_i}^n = \hat{P}(\vec{R} = \vec{r}_*|\Theta = \theta_i) = \frac{m_i}{m} \tag{4.6}$$

where $m = \sum_{j=1}^{n} m_j$.

If the size of realization $\vec{r}_*$ is big, the number of simulations required to obtain reliable estimations can be large. Since the estimations for different source node candidates are independent, the computations can be parallelised.

Additionally for the SIR model, a prunning mechanism can be incorporated. If a sampling simulation infects a node that was not infected during the target epidemic represented by the realization r_*, it is safe to stop the sampling simulation prior to ending time T and call a sample unequal to target realization r_*.

The accuracy of direct Monte Carlo approximations are controlled by convergence conditions. Upon estimating two source PDF's, $\hat{P}_i^n$ and $\hat{P}_i^{2n}$ with n and $2n$ independent simulations, respectively. The PDF's are said to converge when the following conditions are satisfied:

$$|\hat{P}_i^{2n} - \hat{P}_i^n|/\hat{P}_{2n} \leq c, \ |\hat{P}_i^{2n} - \hat{P}_i^n| \leq c \quad \forall \theta_i \in S. \tag{4.7}$$

Algorithm 3: Direct Monte Carlo estimation m_i of expected number of realization hits completely corresponding to r_* for a fixed source θ_i.

```
Data: G - network, $(p, q)$ - parameters of the SIR process, $\vec{r}_*$ - target
      realization, $T$ - temporal threshold, $\theta_i$ - proposed initial source node, $n$ -
      number of simulations
Result: $m_i$ - estimated expected number of realizations started from $\theta_i$ and
        completely corresponding to $r_*$
$m_i = 0$;
for $s = 1$ to $n$ do
    for $t = 1$ to $n$ do
        Run one SIR simulation $(p, q, \theta_i)$ for time step $t$ and obtain $r_i^t$.;
        if $\exists j \in N : (r_i^t(j) == 1$ and $r_*(j) == 0)$ then
            break;
        end
    end
    if $r_i^T$ equals $r_*$ then
        $m_i = m_i + 1$;
    end
end
return $m_i$
```

4.2. The Soft Margin estimator

Let $\vec{r}_{\theta_i}^{(j)}$ denote j-th sample (outcome) obtained by Monte Carlo simulation of contagion process with source node θ_i and duration of T time steps. $\vec{r}_{\theta_i}^{(j)}$ is one realization of random binary vector $\vec{R}_{\theta_i}$ that describes the outcome of epidemic process. A similarity measure $\varphi : (\vec{R}_{\theta_i} \times \vec{R}_{\theta_i}) \to [0, 1]$ can be defined between any two realizations of $\vec{R}_{\theta_i}$, for example, as the Jaccard similarity function:

$$\varphi(\vec{r}_1, \vec{r}_2) = \frac{\vec{r}_1 \cap \vec{r}_2}{\vec{r}_1 \cup \vec{r}_2} = \frac{\sum_{j=1}^{N}(r_1(j) = 1 \text{ and } r_2(j) = 1)}{\sum_{j=1}^{N}(r_1(j) = 1 \text{ or } r_2(j) = 1)}. \tag{4.8}$$

Moreover, we can define a discrete random variable $\varphi(\vec{r}_*, \vec{R}_\theta)$ that measures the similarity between a fixed realization r_* and a random realization from $\vec{R}_\theta$. Let PDF of that random variable be $f_\theta(x)$ where $x = \varphi(\vec{r}_*, \vec{r}_\theta)$. Unbiased estimator for PDF can be obtained with Monte Carlo method from n samples as

$$f_\theta(x) = \int_0^1 p_k \delta(x - x_k) dx \approx \frac{1}{n} \sum_{i=1}^{n} \delta(x - \varphi(\vec{r}_*, \vec{r}_\theta^{(i)})) \tag{4.9}$$

where $\delta(x)$ denotes the Dirac delta function. In the integral we observe a series of probabilities $p_1, p_2, \ldots, p_d$ corresponding to each realization of $\varphi(\vec{r}_*, \vec{R}_\theta)$. With Monte Carlo method, we observe the PDF definition as an integration problem and sample from this discrete distribution $\{p_1, \ldots, p_d\}$ to obtain an estimate.

The Soft Margin estimator is defined as

$$\hat{P}(\vec{R} = \vec{r}_* | \Theta = \theta) = \int_0^1 w_a(x) \hat{f}_\theta(x) dx \tag{4.10}$$

where $w_a(x)$ is a weighting function and $f_\theta(x)$ is the PDF function of the random variable $\varphi(\vec{r}_*, \vec{R}_\theta)$. For $w_a(x)$, [7] proposed a Gaussian weighting form $w_a(x) = e^{-(x-1)^2/a^2}$. In this way, the problem definition was altered to estimating the number of relizations with similarity in the interval defined by Gaussian function $w_a(x)$ around $\varphi = 1$, whereas estimating the number of realizations with similarity strictly equal to $\varphi = 1$ as with Direct Monte Carlo method. In the limit where $a \to 0$ unbiased direct Monte Carlo estimate is obtained.

The Soft Margin formula (4.10) can be further simplified combining with (4.9):

$$\begin{aligned} \hat{P}(\vec{R} = \vec{r}_* | \Theta = \theta) &= \int_0^1 w_a(x) \hat{f}_\theta(x) dx \\ &= \int_0^1 w_a(x) \frac{1}{n} \sum_{i=1}^{n} \delta(x - \varphi(\vec{r}_*, \vec{r}_\theta^{(i)})) dx, \end{aligned} \tag{4.11}$$

and further by using the property of delta distribution $\int_{-\infty}^{\infty} f(x)\delta(x - b)dx = f(b)$:

$$\begin{aligned} \hat{P}(\vec{R} = \vec{r}_* | \Theta = \theta) &= \frac{1}{n} \sum_{i=1}^{n} \int_0^1 w_a(x) \delta(x - \varphi(\vec{r}_*, \vec{r}_\theta^{(i)})) dx \\ &= \frac{1}{n} \sum_{i=1}^{n} w_a(\varphi(\vec{r}_*, \vec{r}_\theta^{(i)})) \\ &= \frac{1}{n} \sum_{i=1}^{n} e^{\frac{(\varphi_i - 1)^2}{a^2}}. \end{aligned} \tag{4.12}$$

Note that it’s not needed to determine constant a in advance. The parameter a can be chosen as the infinum of the set of parameters for which the source probability distribution estimates $\hat{P}_a(\Theta = \theta_i|\vec{R} = \vec{r}_*)$ have converged under the convergence property from (4.7).

Algorithm 4: Soft Margin estimation of $P(\vec{R} = \vec{r}_*|\Theta = \theta_i)$ for a fixed source θ_i.

```
Data: G - network, $(p, q)$ - parameters of the SIR process, $\vec{r}_*$ - target realization,
      $T$ - temporal threshold, $\theta_i$ - proposed initial source node, $n$ - number of
      simulations, $a$
Result: $\hat{P}_a(\vec{R} = \vec{r}_*|\Theta = \theta_i)$
for $s = 1$ to $n$ do
    Run SIR simulation $(p, q, \theta_i)$ for $T$ time steps and obtain $\vec{r}_i^T$;
    Calculate and save $\varphi_i = \varphi(\vec{r}_*, \vec{r}_i^T)$;
end
Calculate $\hat{P}(\vec{R} = \vec{r}_*|\Theta = \theta_i) = \frac{1}{n} \sum_{i=1}^{n} e^{\frac{-(\varphi_i - 1)^2}{a^2}}$;
return $\hat{P}(\vec{R} = \vec{r}_*|\Theta = \theta_i)$
```

4.3. Time complexity of estimators

5. Sequential Importance Sampling estimator

5.1. Importance sampling

Importance sampling is a technique for estimating properties of a particular distribution with samples generated from a different distribution than the one of interest. The technique is used with Monte Carlo method as a variance reduction technique since we usually choose to sample from the distribution that is biased towards the realizations that have more impact on the parameters being estimated.

In other words, the method of importance sampling is estimation of integration problem (4.3) based on generating a sample $X_1, \ldots, X_m$ from a given biased distribution g when in fact the samples X_i come from the target distribution *f*:

$$\mathbf{E_f}[h(X)] = \int_X h(x)f(x)dx = \int_X h(x)\frac{f(x)}{g(x)}g(x)dx \approx \frac{1}{m}\sum_{j=1}^{m}\frac{f(X_j)}{g(X_j)}h(X_j). \tag{5.1}$$

By choosing to sample from the biased distribution g, we are left with the extra weight $w^{(i)} = \frac{f(X_j)}{g(X_j)}$ from the integral that corrects the bias of the estimation. The new estimator converges whatever the choice of distribution g, as long as $supp(g) \supset supp(f)$[1].

Note the estimation can be done with unbiased estimate,

$$\frac{1}{m}\sum_{i=1}^{m} w^{(i)}h(\mathbf{x}^{(i)}), \tag{5.2}$$

or with a weighted estimate

$$\frac{\sum_{i=1}^{m} w^{(i)}h(\mathbf{x}^{(i)})}{\sum_{i=1}^{m} w^{(i)}}. \tag{5.3}$$

When using the weighted estimate, we only need to know the ratio $f(\mathbf{x})/g(\mathbf{x})$ up to a multiplicative constant. Although inducing a small bias, the weighted estimate often has a smaller mean squared error than the unbiased one.

[1] $supp(g) = \{x|g(x) \neq 0\}$

5.1.1. Measuring the quality of importance distribution

By properly choosing $g(\cdot)$, one can reduce the variance of the estimate substantially. In order to make the estimation error small, one wants to choose $g(\mathbf{x})$ as close in shape to $f(\mathbf{x})h(\mathbf{x})$ as possible. The efficiency of such method is difficult to measure. Effective sample size (ESS) is commonly used to measure how different the importance distribution is from the target distribution.

Suppose we have m independent samples generated from $g(\mathbf{x})$. The ESS of this method is defined as

$$\mathrm{ESS}(m) = \frac{m}{1 + var_g[w(\mathbf{x})]}. \tag{5.4}$$

The variance here is estimated as a square of the coefficient of variation of the weights:

$$cv^2 = \frac{\sum_{j=1}^{m}(w^{(j)} - \bar{w})^2}{(m-1)\bar{w}^2}$$

where $\bar{w}$ is sample average of the $w^{(j)}$. The ESS measure of efficiency can be partially justified by the delta method [12].

5.1.2. Rejection control and weighting

When applying importance sampling, one often produces random samples with very small importance weights because of a less than ideal importance density. The following technique for combining rejection and importance weighting can be used.

Suppose we have drawn samples $\mathbf{x}^{(1)}, \ldots, \mathbf{x}^{(m)}$ from $g(\mathbf{x})$. Let $w^{(j)} = \frac{f(\mathbf{x}^{(j)})}{g(\mathbf{x}^{(j)})}$. We can conduct the following operation for any given threshold value $c > 0$:

Algorithm 5: Rejection Control (RC)

```
Rejection Control (RC)
for $j = 1, \ldots, m$, do
    accept $\mathbf{x}^{(j)}$ with probabilty $r^{(j)} = \min\left\{1, \frac{w^{(j)}}{c}\right\}$
    if $\mathbf{x}^{(j)}$ is accepted then
        weight $w^{(j)}$ is updated to $w^{(*j)} = q_c w^{(j)}/r^{(j)}$, where
            $$q_c = \int \min\left\{1, \frac{w^{(j)}}{c}\right\} g(\mathbf{x})d\mathbf{x} \tag{5.5}$$
    end
end
```

Since the constant q_c is the same for all accepted samples, it is not needed for the evaluation of the weighted estimate in (5.3). Nevertheless, it can be unbiasedly estimated [12] from the sample as

$$\hat{p}_c = \frac{1}{m}\sum_{j=1}^{m} \min\Big\{1, \frac{w^{(j)}}{c}\Big\}. \tag{5.6}$$

With this technique we are adjusting the importance density g in light of current importance weights. The new importance density $g^*(\mathbf{x})$ is expected to be close to the target distribution $f(\mathbf{x})$.

After applying rejection control, we will typically have fewer than N samples. More samples can be drawn from either $g(x)$ or $g^*(x)$ (via rejection control) to make up for the rejected samples.

5.2. Sequential importance sampling

Since it is not trivial to design a good importance sampling distribution, especially for high dimensional problems, one may build up the importance density sequentially. Suppose we can decompose $\mathbf{x}$ as $\mathbf{x} = (x_1, \dots, x_d)$ where each of the x_j may be multidimensional. Then our importance distribution can be constructed as

$$g(\mathbf{x}) = g_1(x_1)g_2(x_2|x_1)g_3(x_3|x_1, x_2)\dots g_d(x_d|x_1, \dots, x_{d-1}) \tag{5.7}$$

by which we hope to obtain some guidance from the target density while building up the importance density. We can then rewrite the target density as

$$f(\mathbf{x}) = f_1(x_1)f_2(x_2|x_1)f_3(x_3|x_1, x_2)\dots f_d(x_d|x_1, \dots, x_{d-1}) \tag{5.8}$$

and the weights as

$$w(\mathbf{x}) = \frac{f_1(x_1)f_2(x_2|x_1)f_3(x_3|x_1, x_2)\dots f_d(x_d|x_1, \dots, x_{d-1})}{g_1(x_1)g_2(x_2|x_1)g_3(x_3|x_1, x_2)\dots g_d(x_d|x_1, \dots, x_{d-1})} \tag{5.9}$$

which suggests a recursive monitoring and computing of importance weight:

$$w_t(\mathbf{x}_t) = w_{t-1}(\mathbf{x}_{t-1})\frac{f(x_t|\mathbf{x}_{t-1})}{g(x_t|\mathbf{x}_{t-1})}. \tag{5.10}$$

At the end, w_d is equal to $w(\mathbf{x})$. By using the recursive process we can stop generating further components of $\mathbf{x}$ if the partial weight derived from the sequentially generated partial sample is too small and we can take advantage of $f(x_t|\mathbf{x}_{t-1})$ in designing $g_t(x_t|\mathbf{x}_{t-1})$.

The sequential importance sampling method can then be defined as follows:

Algorithm 6: SIS Step

```
1. Draw $X_t = x_t$ from $g_t(x_t|\mathbf{x_{t-1}})$, and let $\mathbf{x}_t = (\mathbf{x}_{t-1}, x_t)$.
2. Compute $w_t(\mathbf{x}_t) = w_{t-1}(\mathbf{x}_{t-1})\frac{f(x_t|\mathbf{x}_{t-1})}{g(x_t|\mathbf{x})_{t-1})}$.
```

When we observe that w_t is getting too small, we can choose to reject the sample halfway and restart again.

5.2.1. Improving the SIS procedure - rejection control

The rejection control method **RC** can be applied dynamically to improve the **SIS** scheme. Suppose a sequence of "check points," $0 < t_1 < t_2 < \ldots < t_k \leq d$ and a sequence of threshold values $c_1, \ldots, c_k$, are given in advance.

- At each check point t_j start **RC**(t_k) with the threshold value $c = c_j$. If the partial sample $(x_1, \ldots, x_{t_j})$ has a weight w_{t_j}, we accept it with probability $\min\{1, w_{t_j}/c_j\}$. If accepted, replace its weight by $w^*_{t_j} = \max\{w_{t_j}, c_j\}$
- For each rejected partial sample, restart from the beginning again and let it pass through all the check points.

5.2.2. Improving the SIS procedure - resampling

When the system grows, the variance of the importance weights w_t increases. After a certain number of steps, many of the weights become very small and a few very large. In that situation one may use a **resampling** strategy.

Suppose at step t we have a collection of m partial samples of length $t, S_t = \{\mathbf{x}_t^{(j)}, j = 1, \ldots, m\}$ which are properly weighted by the collection of weights $W_t = \{w_t^{(j)}, j = 1, \ldots, m\}$ with respect to the density g.

The resampling step is done on the existing partial sample set before expanding with the **SIS step**.

Simple random sampling

- Sample a new set of partial samples, S'_t from S_t according to the weights $w_t^{(j)}$.
- Assign equal weights, W_t/m, to the samples in S'_t where $W_t = w_t^{(1)} + \ldots + w_t^{(m)}$

Residual resampling

- Retain $k_j = [mw_t^{(*j)}]$ copies of $\mathbf{x}_t^{(j)}$ where $w_t^{(*j)} = w_t^{(j)}/W_t$ and $j = 1, \ldots, m$. Let $m_r = m - k_1 - k_2 - \ldots - k_m$.
- Obtain m_r draws from S_t with probabilities proportional to $mw_t^{(*j)} - k_j$, $j = 1, \ldots m$.
- Reset all the weights to W_t/m.

Residual sampling dominates the simple random sampling in having smaller Monte Carlo variance.

General resampling strategy

- For $j = 1, \ldots m$:

  Draw $\tilde{\mathbf{x}}_t^{(j')}$ independently from the current sample $\{\mathbf{x}_t^{(j)}, j = 1, \ldots, m\}$ according to the probability vector $(a^{(1)}, \ldots, a^{(m)})$. Suppose we obtain $\tilde{\mathbf{x}}^{(j')} = \mathbf{x}_t^{(j)}$.

  A new weight $\tilde{w}_t^{(j')} = w_t^{(j)}/a^{(j)}$ is assigned to this sample.

The new set thus formed is also properly weighted by new weights with respect to g. Because the role of resampling is to prune away "bad" samples and to split the good ones, we should choose $a^{(j)}$ as a monotone function of $w_t^{(j)}$. We can choose $a^{(j)}$ to reflect certain future trend, balance between the need of diversity and the of focus (giving more presence to the samples with large weights) etc. A generic choice is $a^{(j)} = [w_t^{(j)}]^{\alpha}$ with $0 < \alpha \leq 1$ that can vary according to the variance of w_t.

Resampling schedule

The resampling step tends to result in a better group of anecestors so as to produce better descendants. The success of resampling, however, relies heavily on the Markovian structure among the state variables $x_1, x_2, \ldots$. Given the realization of x_t, the next variable x_{t+1} is statistically independent of all the previous states $\mathbf{x}_{t-1}$. If the resampling from set $\{\mathbf{x}_{t-1}^{(j)}, j = 1, \ldots m\}$ is not equivalent to resampling from $\{x_{t-1}^{(j)}, j = 1, \ldots, m\}$, the set of the "current state" frequent resampling will rapidly impoverish diversity of the partial samples produced earlier. When no simple Markovian structure is present, frequent resampling generally gives bad results.

For this reason, it is desirable to prescribe a schedule for the resampling to take place. The resampling schedule can be either deterministic or dynamic. When the schedule is dynamic, some small bias may be introduced.

With a deterministic schedule, we conduct resampling at time $t_0, 2t_0, \ldots,$ where t_0 is given in advance. In a dynamic schedule, a sequence of thresholds $c_1, c_2, \ldots,$ are given in advance. We monitor the coefficient of variation of the weights cv_t^2 and invoke the resampling step when event $cv_t^2 > c_t$ occurs. A typical sequence of c_t can be $c_t = a + bt^\alpha$.

Increasing c_t after each SIS step makes sense since it can be shown that as the system evolves, cv_t^2 increases stochastically [13].

Resampling scheme

- Check the weight distribution by performing one of the methods at time t. Resample if needed.
- Invoke an SIS step. Set $t = t + 1$.

5.2.3. Partial rejection control

As t increases, cv_t^2 increases stochastically and the weights w_t typically become skewed. As a consequence, many samples will have minimal impact on the final estimation. It is thus desirable to prune them away at an earlier stage. In 5.2.1 we have seen how the rejection control method can be used to achieve pruning without creating bias or correlations. However, the implementation of full rejection control requires that we make up the lost samples by restarting from stage 1 and passing through all the intermediate rejection steps. Instead of employing the full rejection control, we can follow a more pratical, partial rejection method that combines both rejection and resampling.

Partial rejection control

- At each check point t_k, start **RC**(t_k) from 5 with threshold value $c = c_k$. If the stream $\mathbf{x}_{t_k}^{(j)}$ passes this check point, we proceed with standard SIS replacing the old weight with $w_{t_k}^{(*j)} = \max\{w_{t_k}^{(j)}, c_k\}$.
- When rejected, go back to check point t_{k-1} to draw a sample $x_{t_{k-1}}^{(j)}$ from the sample pool $S_{t_{k-1}}$, with probability proportional to $w_{t_{k-1}}^{(j)}$. Reset its weight to $\bar{w}_{t_{k-1}}$ and make a SIS step. If the new sample formed in this way pass the check point t_k, then its weight is set as $w_{t_k}^{(*j)} = \max\{w_{t_k}^{(j)}, c_k\}$
- Reset all the weights to $w_{t_k}^{(j)} = \hat{p}_c w_{t_k}^{(*j)}$.

5.3. Sequential Importance sampling estimator

Given snapshot r_* that holds all infected nodes up to time T, we want to determine the probability of epidemic starting in node θ_i, $P(\theta_i|\vec{S} = \vec{s}_*)$ where $\vec{R}$ is a random variable whose one realization is $\vec{s}_*$. Since all the apriori probabilities $P(\theta_i)$ are the same, we can approximate aposteriori probabilities $P(\vec{S} = \vec{s}_*|\theta_i)$ and use then to determine $P(\theta_i|\vec{S} = \vec{s}_*)$:

$$\hat{P}(\theta_i|\vec{S} = \vec{s}_*) = \frac{\hat{P}(\vec{S} = \vec{s}_*|\theta_j)}{\sum_j \hat{P}(\vec{S} = \vec{s}_*|\theta_j)}$$

The aposteriori probabilities are estimated with Direct Monte Carlo and Soft Margin method up to a multiplicative constant. This can also be done using Sequential Importance Sampling.

First note the **SIS step** as defined in 6 is based on the densities of a complete history of the process, or at time t, all the process steps up to time t. The target density is thus the join probability of all the steps taken in the process. Since we are only interested in the final realization, it makes sense to use target (and importance) density of the form:

$$f(s_t) = f_1(i_1, r_1)f_2(i_2, r_2|i_1, r_1)f_3(i_3, r_3|i_2, r_2)\dots f_t(i_t, r_t|i_{t-1}, r_{t-1})$$

$$g(s_t) = g_1(i_1, r_1)g_2(i_2, r_2|i_1, r_1)g_3(i_3, r_3|i_2, r_2)\dots g_t(i_t, r_t|i_{t-1}, r_{t-1}))$$

where i_t denotes a vector of infected nodes at time t, and r_t denotes a vector of recovered nodes at time t. Note that $(i_t, r_t) = s_t$. The sequence $(i_1, r_1), (i_2, r_2), (i_3, r_3), \dots, (i_t, r_t)$ is connected with a SIR step.

5.3.1. Modelling the target distribution

We can evaluate the partial target density $f_k(i_k, r_k|i_{k-1}, r_{k-1})$ in closed form. Denote as $nei(v)$ a set of all neighbours of node v, as $nei(I)$ a set of all neighbours of all nodes in I and as $nei_I(v) = nei(v) \cap I$ a set of all neighbours of v that are in I. One step SIR simulation was conducted and the resulting i_k and r_k were given. For each node v in $i_{k-1} \cup nei(i_{k-1})$, 1 of 4 independent events may have happened:

- if $v \in i_{k-1}$ and $v \in r_k$ node v was recovered with probability q.
- if $v \in i_{k-1}$ and $v \notin rk$ node v was not recovered with probability $1 - q$.
- if $v \notin i_{k-1}$ and $v \in i_k$ node v was infected with probability $1 - (1-p)^{nei_{i_{k-1}}(v)}$
- if $v \notin i_{k-1}$ and $v \notin i_k$ node v was not infected with probability $(1-p)^{nei_{i_{k-1}}(v)}$

Since all the events are independent, the target density is of the form

$$f_k(i_k, r_k|i_{k-1}, r_{k-1}) = \left[\Pi_{v\in E_1} q\right]\left[\Pi_{v\in E_2}(1-q)\right]\left[\Pi_{v\in E_3}(1-(1-p)^{nei_{i_{k-1}}(v)})\right]\left[\Pi_{v\in E_4}(1-p)^{nei_{i_{k-1}}(v)}\right].$$

5.3.2. Modelling the importance distribution

With our sequential sampling procedure we will try to estimate the number of realizations at time T that are equal to $s*$. The importance density will be biased towards that goal. Since we are building the final densities sequentially, our biased sampling must sample reasonably enough at each step (it must not be to "slow" or too "fast"), especially since it is not certain what samples at mid steps are valuable too us as we might perform some sort of resampling or reduction.

It is certain, however, we do not want to infect the nodes that were never infected in the snapshot $s*$ and we can safely use $SIR(p = 1, q)$ at the last **SIS** step. That leads us to the biased density similar to f where only the nodes in $s*$ are eligible for events E_3, E_4 and it holds $p = 1$ when $k = T$.

It may be reasonble to increase p at each step of **SIS** procedure but it is not clear when this should be done. Additionally, one might want to use a resampling or a rejection technique based on vc^2 for simulations with many **SIS** steps. This has to be done carefully too since our target event is rare and weights w are naturally small.

6. Benchmark dataset

Antulov-Fantulin et al. [7] provided a dataset of SIR realizations along with their estimations obtained with Direct Monte Carlo for 4 classes of SIR parameters: $A = (p = 0.3, q = 0.3, T = 0.5), B = (p = 0.3, q = 0.7, T = 0.5), C = (p = 07, q = 0.3, T = 5)$ and $D = (p = 0.7, q = 0.7, T = 5)$. The benchmark dataset contains 160 such realizations on the grid of size $30x30$. Their estimations obtained with Direct Monte Carlo were held under convergence condition $|P_{ML}^{2n} - P_{ML}^{n}|/P_{ML}^{2n}| \leq 0.05$ and $|P_i^x - P_i^{2x}| \leq 0.05$ for all other nodes.

6.1. Correctness of the Direct Monte Carlo implementation

6.2. Correctness of the Soft Margin implementation

For the Soft Margin estimator we use the following convergence condition:

$|\hat{P}_a^n(\Theta = \theta_{MAP}|\vec{R} = \vec{r}_*) - \hat{P}_a^{2n}(\Theta = \theta_{MAP}|\vec{R} = \vec{r}_*)|/\hat{P}_a^{2n}(\Theta = \theta_{MAP}|\vec{R} = \vec{r}_*) \leq 0.05$

and

$$|\hat{P}_a^n(\Theta = \theta|\vec{R} = \vec{r}_*) - \hat{P}_a^{2n}(\Theta = \theta|\vec{R} = \vec{r}_*)| \leq 0.05.$$

6.3. Sequential Importance Sampling results

Sequential importance sampling is done under importance sampling distribution with the following properties:

- parameter p is fixed in steps $t < 5$ and $p = 1$ in the last step $t = T = 5$,
- parameter q is fixed,
- at each step, only nodes that are in the given final simulation may be infected with probability p,

- nodes that are infected may be recovered with probability q.

The simulations are done under the same convergence condition as Direct Monte Carlo simulation from the benchmark dataset, starting from $n = 10000$ samples.

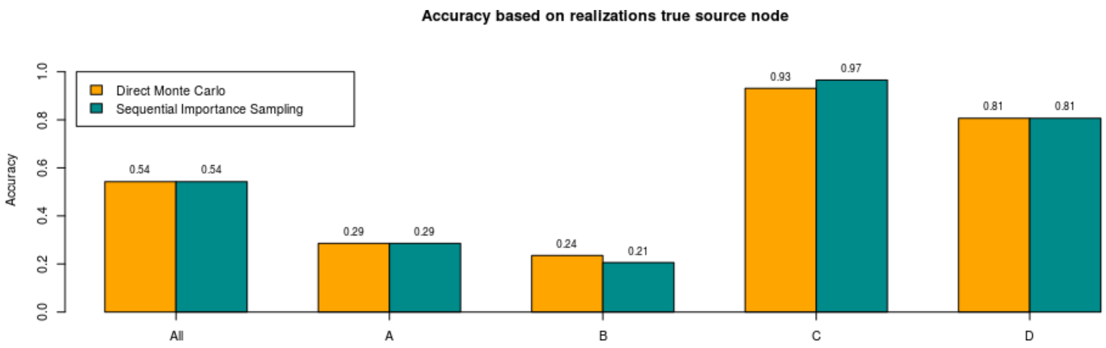

Figure 6.1

Figure 6.1 represents accuracies of estimations obtained by Direct Monte Carlo and Sequential Importance Sampling estimators w.r.t. the realizations true source node. In other words, they represent the portion of MAP estimations that correctly estimated the source node of the realization. When we observe low accuracy for Direct Monte Carlo estimator on average, we shouldn't expect such accuracy to be higher for the "inferior" Sequential Monte Carlo estimator. Accuracies for Direct Monte Carlo and Sequential Importance Sampling estimators follow similar pattern overall and for all the SIR parameter classes. For classes A and B they are low, and for classes C and D they are high.

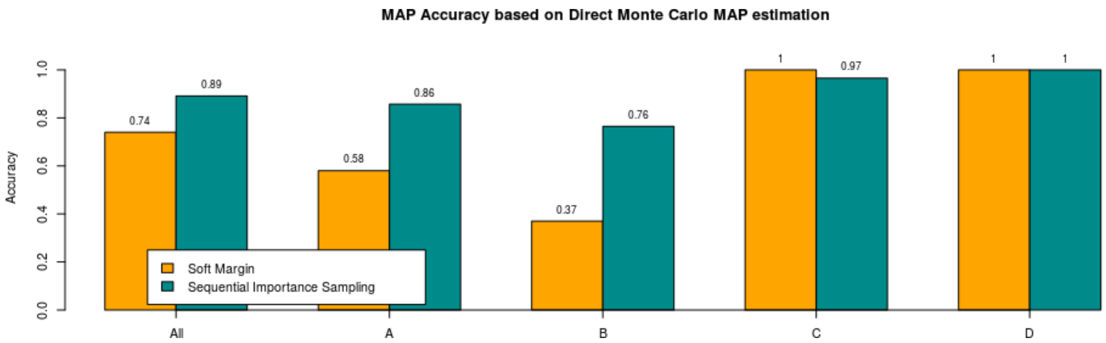

Figure 6.2

Figure 6.2 represents the accuracy used in [7] to compare range of estimators. This accuracy refers to the portion of MAP estimations that are equal to corresponding MAP estimations of Direct Monte Carlo estimator provided in the benchmark dataset. Soft Margin accuracies presented here are taken from [7].Those were calculate with fixed $a = 0.031$ and under the same convergence conditions as the benchmark Direct

Monte Carlo solutions. Sequential Importance Sampling estimator for classes A and B outperforms SoftMargin. This only means its MAP estimations are more similar to Direct Monte Carlo estimations. Note that these classes also have low true source node accuracy and belong to low to medium detectability zone of parameters.

The similarity between estimations obtained with Sequential Importance Sampling and Direct Monte Carlo also presents itself as a low relative MAP error estimation w. r. t. Direct Monte Carlo probability across all classes of parameters, as presented in Figure 6.3.

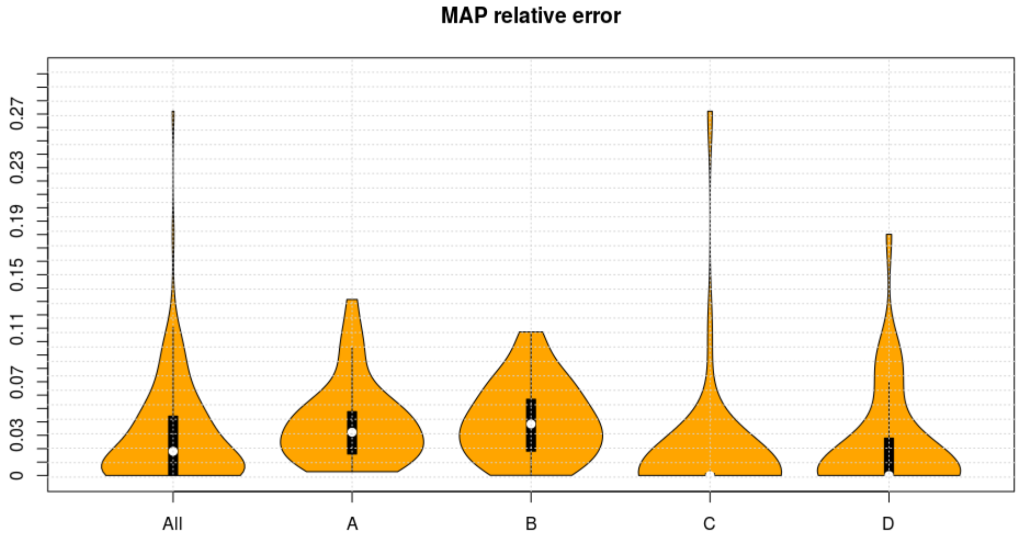

Figure 6.3

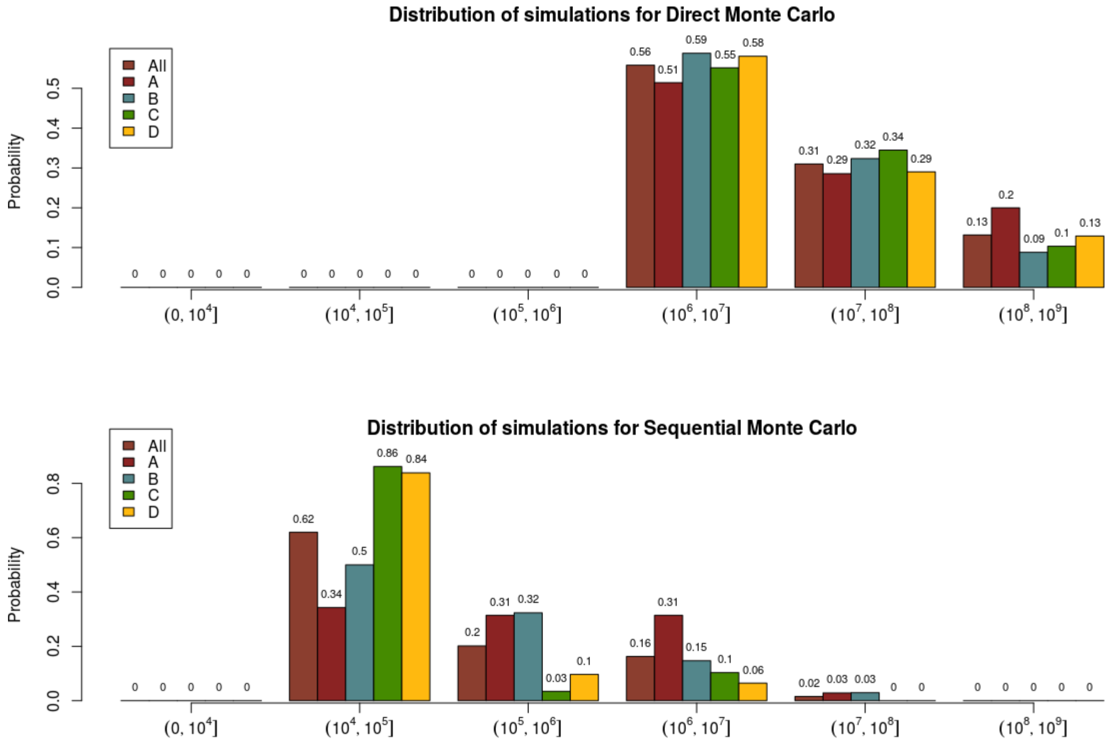

Figure 6.4

In Figure 6.4 distributions of number of simulations (samples) for which the estimators converged are presented. For Sequential Importance Sampling estimator we observe 10^5 samples are needed for SIR parameters in classes C and D in more than 80% of benchmark realizations. However, some simulations, observably mostly those in classes A and B, require more than 10^6 samples for convergence. The impact on the accuracies and the results presented here when the number of samples is capped by 10^6 is yet to be analysed.

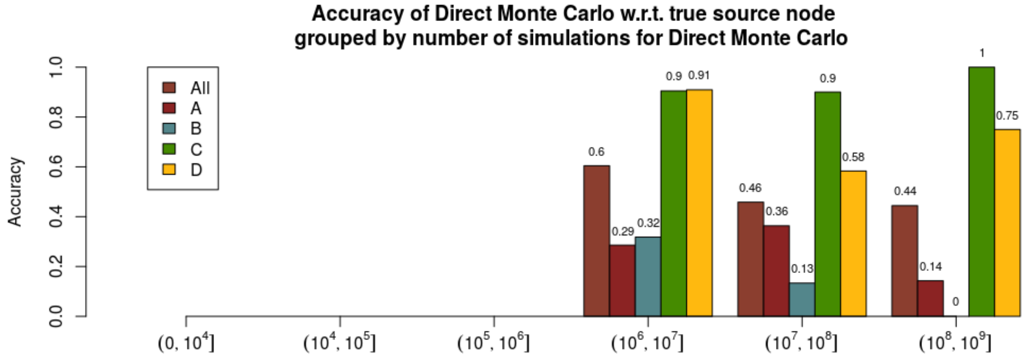

Figure 6.5

Figure 6.5 presents accuracy w.r.t. true source node of Direct Monte Carlo and Sequential Importance Sampling based estimations grouped by number of simulations required to obtain Direct Monte Carlo estimation for the coresponding benchmark sample.

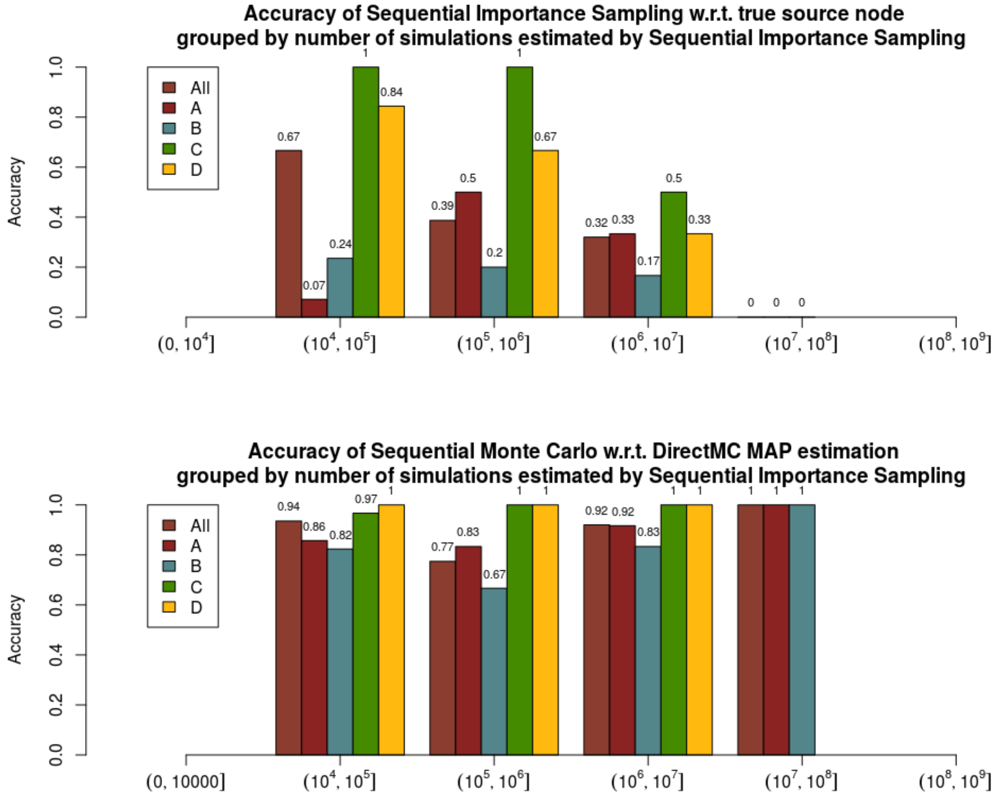

Figure 6.6

Figure 6.6 presents accuracies for Sequential Importance Sampling. Note the benchmark samples that required more than 10^7 simulations are the ones Direct Monte Carlo estimator also failed to estimate correctly.

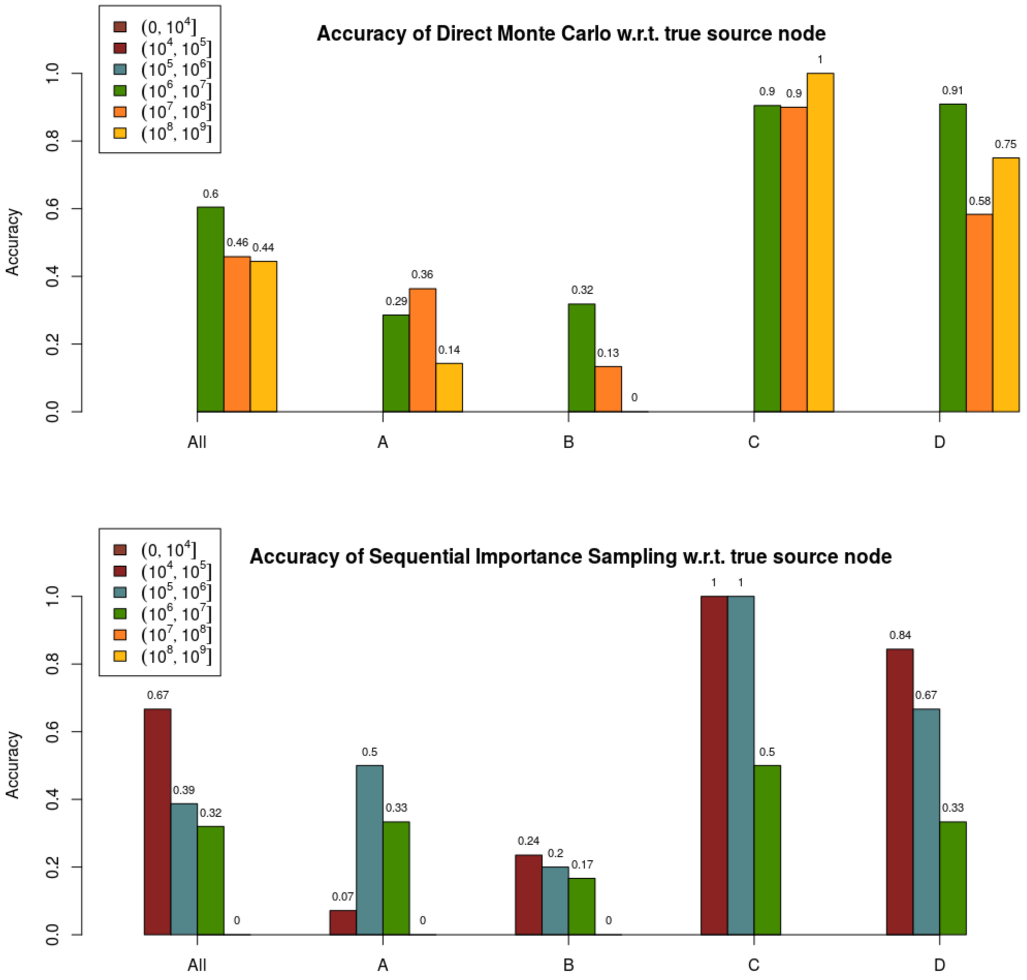

Accuracy of Direct Monte Carlo w.r.t. true source node
(0, 10^4]
(10^4, 10^5]
(10^5, 10^6]
(10^6, 10^7]
(10^7, 10^8]
(10^8, 10^9]
Accuracy
0.0
0.2
0.4
0.6
0.8
1.0
0.6
0.46
0.44
0.29
0.36
0.14
0.32
0.13
0
0.9
0.9
1
0.91
0.58
0.75
All
A
B
C
D
Accuracy of Sequential Importance Sampling w.r.t. true source node
(0, 10^4]
(10^4, 10^5]
(10^5, 10^6]
(10^6, 10^7]
(10^7, 10^8]
(10^8, 10^9]
Accuracy
0.0
0.2
0.4
0.6
0.8
1.0
0.67
0.39
0.32
0
0.07
0.5
0.33
0
0.24
0.2
0.17
0
1
1
0.5
0.84
0.67
0.33
All
A
B
C
D

Figure 6.7

7. Detectability of patient zero

The source detectability $D(\vec{r_*}) = 1 - H(\vec{r_*})$ is characterized via Shannon entropy H (normalized by entropy of uniform distribution) of the estimated source probability distribution $P(\Theta = \theta_i | \vec{R} = \vec{r_*})$.

7.1. Detectability based on parameters of the SIR model

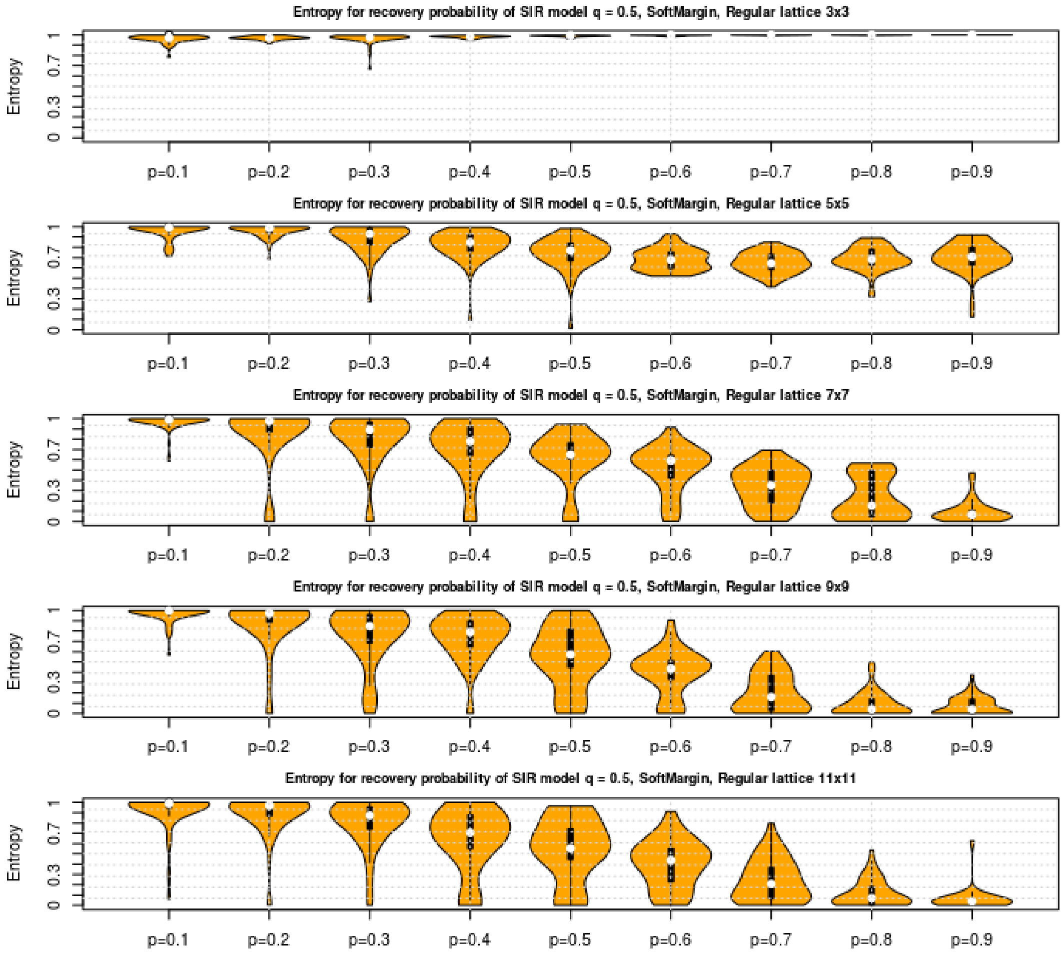

Figure 7.1: Box plots of estimated entropy density for entropy of source probability distributions of single source candidates on the 4-connected lattice of different sizes estimated with Soft Margin method with $10^4 - 10^6$ simulations with adaptive a chosen from $\{1/2^3, 1/2^4, \ldots, 1/2^{15}\}$. Estimation is done under SIR model with different parameters p in range $0.1 - 0.9$, fixed $q = 0.5$ and $T = 5$. The source node in each experiment is the central node of lattice. Each entropy density is estimated with 50 experiments containing realizations with more than 1 node.

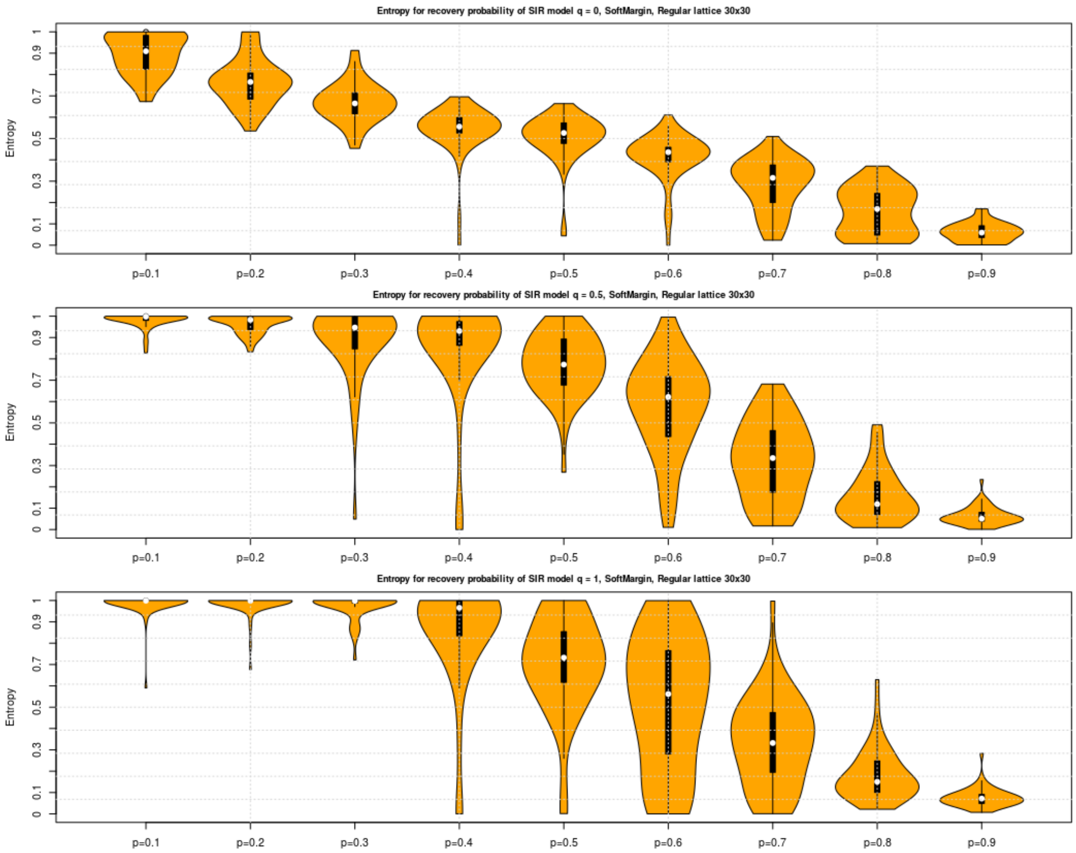

Figure 7.2: Box plots of estimated entropy density for entropy of source probability distributions of single source candidates on the 4-connected lattice 30×30 estimated with Soft Margin method with $10^4 - 10^6$ simulations with adaptive a chosen from $\{1/2^3, 1/2^4, \ldots, 1/2^{15}\}$. Estimation is done under SIR model with different parameters p in range $0.1 - 0.9$, and $q = \{0, 0.5, 1\}$ with $T = 5$. The source node in each experiment is the central node of lattice. Each entropy density is estimated with 50 experiments containing realizations with more than 1 node.

In Figures 7.1 and 7.2 the results of [7] are reproduced. The existence of different detectability regimes is shown in Figure 7.2 as well as a similar detectability behaviour for SIR models with the same parameter p across different values of parameter q. Three entropy regions are observed: low detectability-high entropy region $(p < 0.2)$, intermediate detectability - intermediate entropy region $(0.2 < p < 0.7)$ and high detectability-low entropy region $(p > 0.7)$.

In a regime where network size restricts the epidemic spreading but not the epidemic itself, the entropy is high as the realizations from different sources are almost identical (Figure 7.1).

7.2. Detectability based on parameters of the ISS model

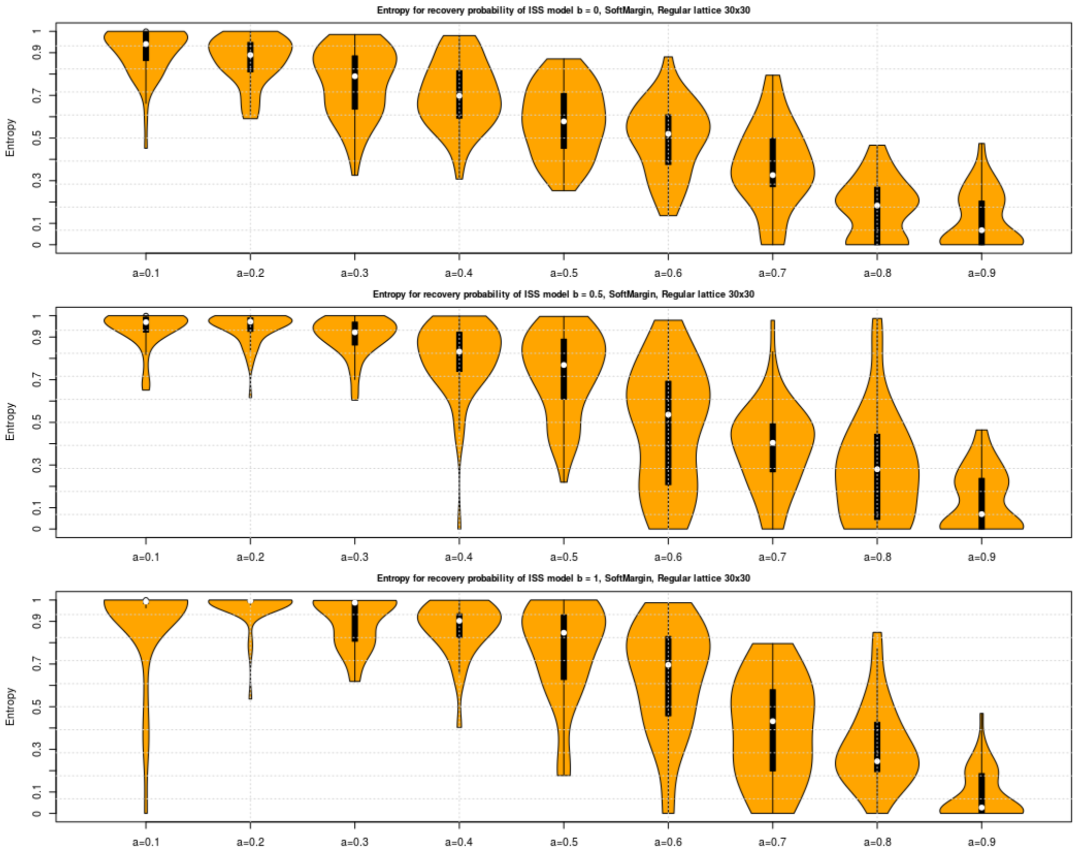

Figure 7.3: Box plots of estimated entropy density for entropy of source probability distributions of single source candidates on the 4-connected lattice 30×30 estimated with Soft Margin method with $10^4 - 10^6$ simulations with adaptive a chosen from $\{1/2^3, 1/2^4, \dots, 1/2^{15}\}$. Estimation is done under ISS model with different parameters a in range $0.1 - 0.9$, and $b = \{0, 0.5, 1\}$ with $T = 5$. The source node in each experiment is the central node of lattice. Each entropy density is estimated with 50 experiments containing realizations with more than 1 node.

7.3. Detectability based on network topology for the SIR model

7.3.1. Barabassi graph

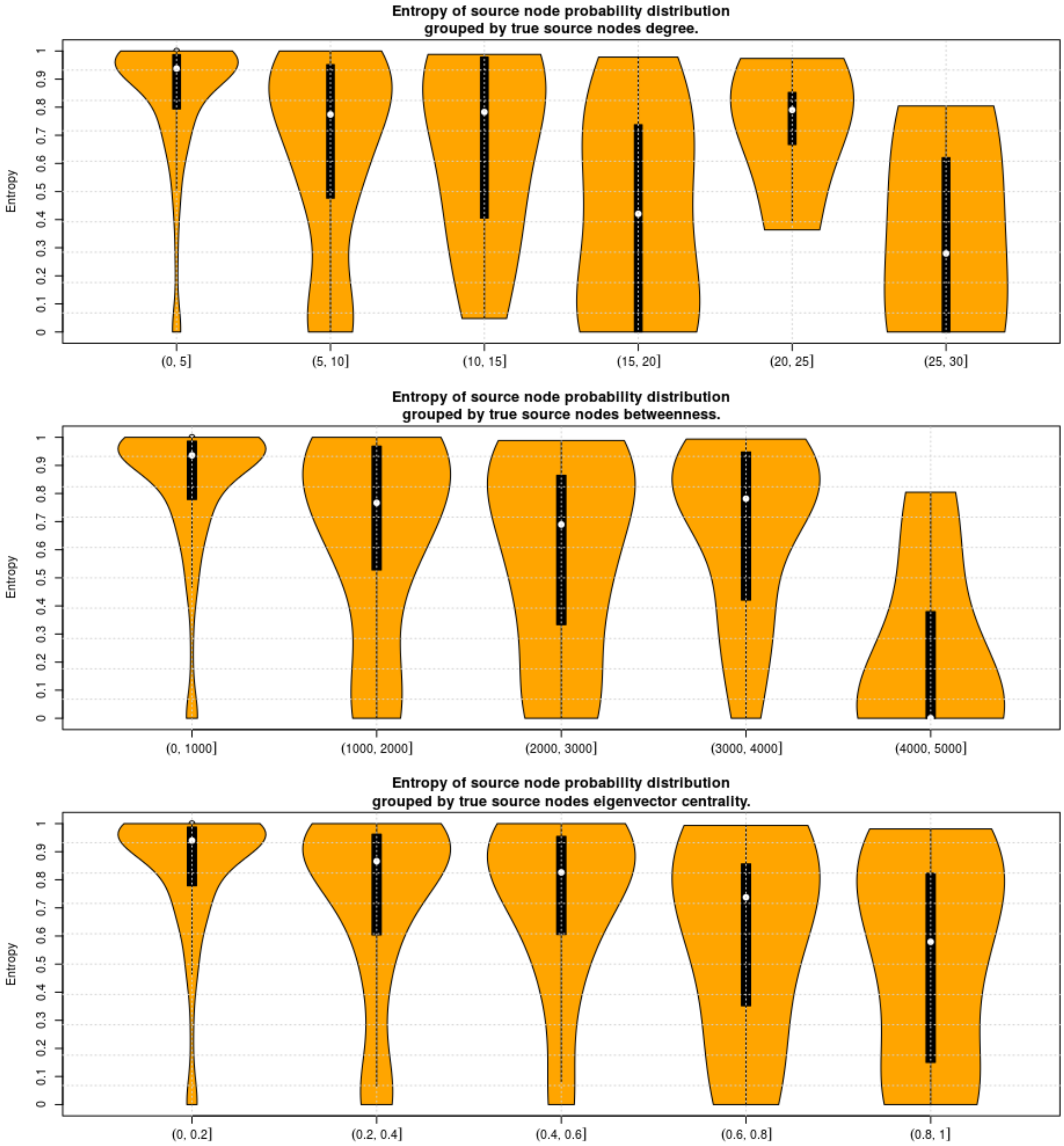

Figure 7.4: Kepsn

7.3.2. Erdos-Renyi graph

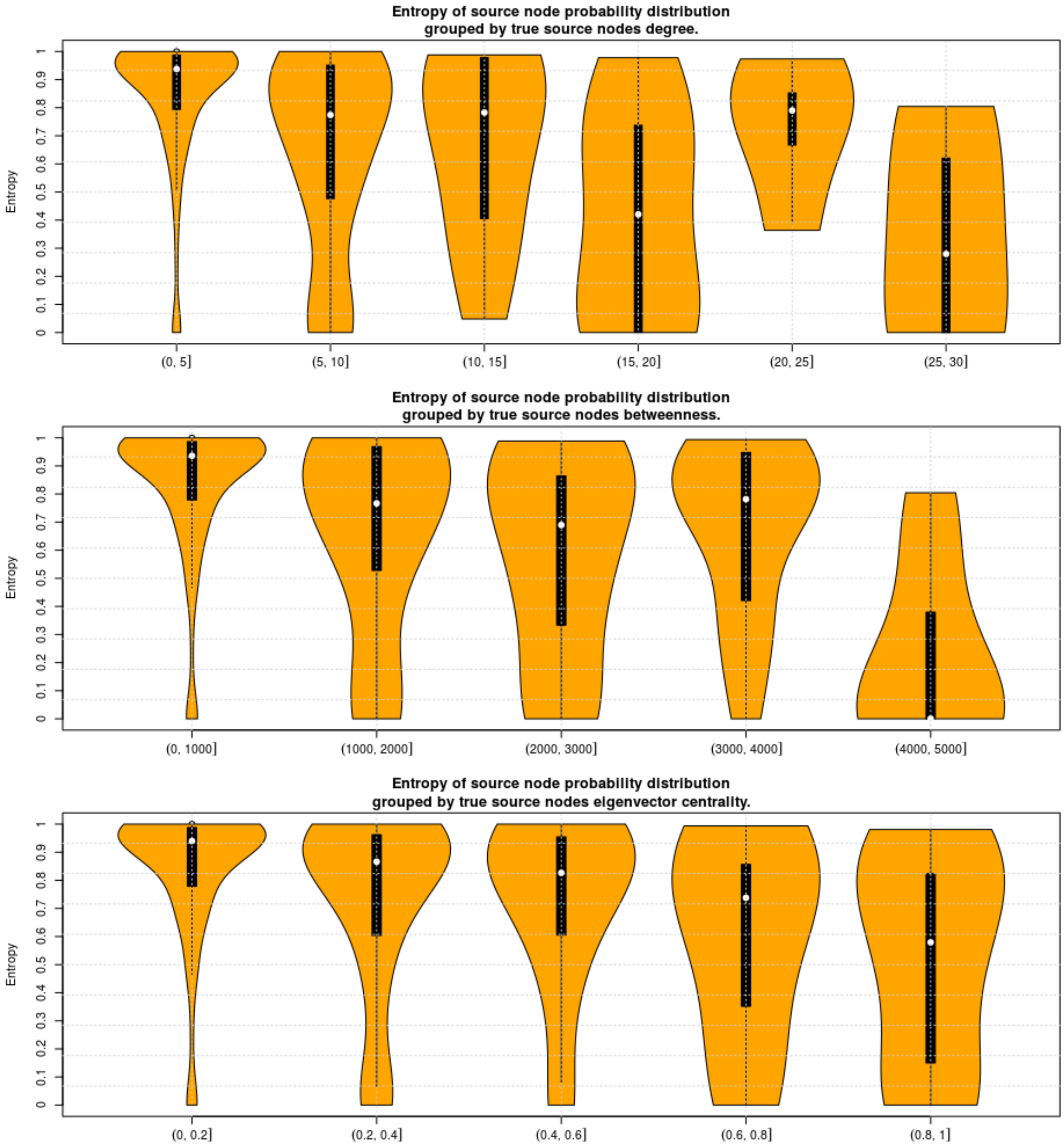

Figure 7.5: Kepsn

7.3.3. Topological properties of the nodes

8. Conclusion

Zaključak.

BIBLIOGRAPHY

[1] Valdis Krebs. The social graph of a facmous mathematician. http://www.orgnet.com/Erdos.html, 2014.

[2] M. E. J. Newman. The structure and function of complex networks. *SIAM REVIEW*, 45:167–256, 2003.

[3] Romualdo Pastor-Satorras, Claudio Castellano, Piet Van Mieghem, and Alessandro Vespignani. Epidemic processes in complex networks. *Rev. Mod. Phys.*, 87:925–979, Aug 2015. doi: 10.1103/RevModPhys.87.925. URL http://link.aps.org/doi/10.1103/RevModPhys.87.925.

[4] Jiaojiao Jiang, Sheng Wen, Shui Yu, Yang Xiang, Wanlei Zhou, and Ekram Hossain. Identifying propagation sources in networks: State-of-the-art and comparative studies. *IEEE Communications Surveys and Tutorials, accepted*, 17(9), 2014.

[5] Kai Zhu and Lei Ying. Information source detection in the SIR model: A sample path based approach. *CoRR*, abs/1206.5421, 2012. URL http://arxiv.org/abs/1206.5421.

[6] Andrey Y. Lokhov, Marc Mézard, Hiroki Ohta, and Lenka Zdeborová. Inferring the origin of an epidemic with a dynamic message-passing algorithm. *Phys. Rev. E*, 90:012801, Jul 2014. doi: 10.1103/PhysRevE.90.012801. URL http://link.aps.org/doi/10.1103/PhysRevE.90.012801.

[7] Nino Antulov-Fantulin, Alen Lančić, Tomislav Šmuc, Hrvoje Štefančić, and Mile Šikić. Identification of patient zero in static and temporal networks: Robustness and limitations. *Phys. Rev. Lett.*, 114:248701, Jun 2015. doi: 10.1103/PhysRevLett.114.248701. URL http://link.aps.org/doi/10.1103/PhysRevLett.114.248701.

[8] Phillip Bonacich. Power and centrality: A family of measures. *American Journal of Sociology*, 92(5):1170–1182, 1987.

[9] J. F. F.; Samukhin A. N. Dorogovtsev, S. N.; Mendes. Structure of growing networks with preferential linking. *Physical Review Letters*, 85, 11 2000. doi: 10.1103/physrevlett.85.4633. URL `http://gen.lib.rus.ec/scimag/index.php?s=10.1103/physrevlett.85.4633`.

[10] Nino Antulov-Fantulin, Alen Lancic, Hrvoje Stefancic, and Mile Sikic. Fastsir algorithm: A fast algorithm for simulation of epidemic spread in large networks by using SIR compartment model. *CoRR*, abs/1202.1639, 2012. URL `http://arxiv.org/abs/1202.1639`.

[11] Yamir Moreno, Maziar Nekovee, and Amalio F. Pacheco. Dynamics of rumor spreading in complex networks. *Phys. Rev. E*, 69:066130, Jun 2004. doi: 10.1103/PhysRevE.69.066130. URL `http://link.aps.org/doi/10.1103/PhysRevE.69.066130`.

[12] Jun S. Liu. *Monte Carlo Strategies in Scientific Computing*. Springer Publishing Company, Incorporated, 2008. ISBN 0387763694, 9780387763699.

[13] Wing Hung Wong Augustine Kong, Jun S. Liu. Sequential imputations and bayesian missing data problems. *Journal of the American Statistical Association*, 89(425):278–288, 1994. ISSN 01621459. URL `http://www.jstor.org/stable/2291224`.

Detectability of Patient Zero Depending on its Position in the Network

Sažetak

Sažetak na hrvatskom jeziku.

Ključne riječi: Ključne riječi, odvojene zarezima.

Title

Abstract

Abstract.

Keywords: Keywords.